Short-range correlations in nuclei with similarity renormalization group transformations

T. Neff,[1,*] H. Feldmeier,[1,2] and W. Horiuchi[3]

[1]*GSI Helmholtzzentrum für Schwerionenforschung GmbH, Planckstraße 1, 64291 Darmstadt, Germany*
[2]*Frankfurt Institute for Advanced Studies, Max-von-Laue Straße 1, 60438 Frankfurt, Germany*
[3]*Department of Physics, Hokkaido University, Sapporo 060-0810, Japan*

Background: Realistic nucleon-nucleon interactions induce short-range correlations in nuclei. To solve the many-body problem unitary transformations like the similarity renormalization group (SRG) are often used to soften the interactions.

Purpose: Two-body densities can be used to illustrate how the SRG eliminates short-range correlations in the wave function. The short-range information can however be recovered by transforming the density operators.

Method: The many-body problem is solved for ^{4}He in the no core shell model (NCSM) with SRG transformed AV8' and chiral N3LO interactions. The NCSM wave functions are used to calculate two-body densities with bare and SRG transformed density operators in two-body approximation.

Results: The two-body momentum distributions for AV8' and N3LO have similar high-momentum components up to relative momenta of about 2.5 fm^{-1}, dominated by tensor correlations, but differ in their behavior at higher relative momenta. The contributions of many-body correlations are small for pairs with vanishing pair momentum but not negligible for the momentum distributions integrated over all pair momenta. Many-body correlations are induced by the strong tensor force and lead to a reshuffling of pairs between different spin-isospin channels.

Conclusions: When using the SRG it is essential to use transformed operators for observables sensitive to short-range physics. Back-to-back pairs with vanishing pair momentum are the best tool to study short-range correlations.

PACS numbers: 21.60.De, 21.30.Fe, 05.10.Cc, 25.30.-c

I. INTRODUCTION

Realistic nucleon-nucleon (NN) interactions are fitted to NN scattering data up to the pion production threshold. Therefore their properties at short distances r and also their off-shell behavior is not completely constrained. All realistic interactions include pions to describe the long- and medium-range parts of the potential. The short-range part is parameterized phenomenologically [1], by the exchange of heavy mesons [2], or in chiral effective field theory by (regularized) contact-terms [3, 4]. At short distances $r \lesssim 1.5$ fm the different interactions induce typical short-range correlations due to short-range repulsion and the tensor force which is reflected in a depopulation of one-body momentum distributions below the Fermi momentum and an enhancement at high momenta when compared to single-particle mean-field occupation probabilities [5–10].

However short-range correlations are two-body correlations and therefore two-body densities in coordinate and momentum space provide the best tool to study these correlations. Experimentally short-range correlations have been studied in inclusive, semi-inclusive and triple-coincidence reactions, see the reviews [11, 12] and references therein. The most direct information about two-body correlations can be obtained in triple-coincidence experiments where one knocks out a nucleon pair with protons [13] or electrons [14–17] at high-momentum transfer. In these experiments one found a dominance of pn over pp pairs at high relative momenta, that indicated the importance of short-range tensor correlations. Tensor correlations also appear to play a major role in (p, d) reactions at high proton energies [18, 19].

Recent theoretical studies of two-body momentum distributions can explain these observations. In a simple picture only close nucleons found in relative S-wave pairs are affected by short-range correlations and in a first approximation high-momentum components are generated by pairs in deuteron-like configurations [20]. The two-body momentum distributions at high momenta can also be connected to the nuclear contacts [21]. Detailed few- and many-body calculations almost exclusively use the Argonne v_{18} (AV18) or Argonne v_8' (AV8') interactions [22–26]. Compared to the Argonne interactions, interactions derived in chiral effective field theory [3] are regularized with a relatively low momentum cut-off and one might expect noticeable differences for the short-range correlations.

From the perspective of nuclear many-body calculations short-range correlations are not a desired feature but pose a severe problem. One way to address this problem is to include the short-range correlations explicitly, as in the correlated basis function theory [27] or in variational Monte Carlo (VMC) calculations [22–24]. Another approach is to use soft phase-shift equivalent effective interactions that are obtained from the bare interactions by means of unitary transformations like V_{low-k} [28], the unitary correlation operator method (UCOM) [8, 29, 30] or the similarity renormalization group (SRG) [30–32]. In real life the unitary transformations are performed in an n-body approximation. This usually means in two-body, or for state of the art SRG calculations, in three-body approximation [33–35]. Even if we only have a two-body interaction at the beginning the unitary transformation will induce three- and higher-body terms. If the unitary transformation acts mainly at short distances and the density of the nuclear system is low enough, so that the probability to find three nucleons simultaneously close together is small, transformations on the two-body level will be a good approximation. The re-

* email: t.neff@gsi.de

maining dependence of observables on the unitary transformation can be used to analyze the nature of missing many-body terms.

In a consistent calculation it is not enough to transform the Hamiltonian, all operators have to be transformed. Within the SRG approach the transformation of long-range operators like radius or electromagnetic transition operators has been studied in [36] in two- and three-body approximation. As one might expect the effect on these long-range operators is not very large. On the other hand we expect large effects for short-range or high-momentum observables. Within the UCOM approach we investigated these effects in two-body approximation and with simple trial wave functions for the one-body momentum distribution [8] and for two-body coordinate and momentum space distributions [37]. The SRG operator evolution for the deuteron was studied extensively in [38] and analyzed in terms of a factorization for high-momentum observables. These ideas were extended for Fermi gases in [39].

In this paper we investigate two-body densities for the ground state of ^{4}He in coordinate and momentum space for SRG transformed AV8' [1] and chiral N3LO [3] interactions using the no core shell model (NCSM). For the bare AV8' interaction the NCSM results are not converged and we use in this case the method of correlated Gaussians [37, 40, 41]. We will discuss the two-body densities obtained with both, bare and transformed density operators. The SRG transformation depends on the flow parameter that controls the softness of the transformed interaction. We perform the SRG transformation in two-body approximation and use the flow-dependence of the results to test the quality of the two-body approximation. We will show that for pairs with vanishing pair momentum the contributions of three-body correlations are negligible.

After describing in Sec. II the used methods, two-body densities in coordinate and momentum space are presented in Sec. III where we also discuss the role of many-body correlations for different observables. Summary and conclusions follow in Sec. IV. Technical details about the calculation of translational invariant two-body densities in the NCSM framework are presented in the Appendix.

II. METHOD

The SRG flow equation for the Hamiltonian $\widehat{H}_\alpha = \widehat{T}_{\rm int} + \widehat{V}_\alpha$ and the corresponding transformation matrix $\widehat{U}_\alpha$ are given by

$$\frac{d\widehat{H}_\alpha}{d\alpha} = [\widehat{\eta}_\alpha, \widehat{H}_\alpha], \quad \frac{d\widehat{U}_\alpha}{d\alpha} = -\widehat{U}_\alpha \widehat{\eta}_\alpha \,, \tag{1}$$

with the generator $\widehat{\eta}_\alpha$ taken to be the commutator of the intrinsic kinetic energy and the evolved Hamiltonian:

$$\widehat{\eta}_\alpha = (2\mu)^2\,[\widehat{T}_{\rm int}, \widehat{H}_\alpha], \quad \widehat{T}_{\rm int} = \widehat{T} - \widehat{T}_{\rm cm} \,. \tag{2}$$

Please note that $\widehat{U}_\alpha$ used here and in Ref. [30] corresponds to $\widehat{U}_s^\dagger$ in Refs. [31, 32].

In this paper the Hamiltonian is transformed in two-body approximation:

$$\widehat{H}_\alpha = \widehat{U}_\alpha^\dagger \widehat{H} \widehat{U}_\alpha = \widehat{T}_{\rm int} + \widehat{V}_\alpha^{[2]} + \ldots + \widehat{V}_\alpha^{[N]} \approx \widehat{T}_{\rm int} + \widehat{V}_\alpha^{[2]} \,. \tag{3}$$

The evolution (1) can therefore be performed for the relative motion in two-body space. The flow equations are solved on a momentum space grid with relative momenta going up to $k_{\rm max} = 15\,{\rm fm}^{-1}$ for the AV8' interaction. In the end the momentum space matrix elements are evaluated in the harmonic oscillator basis to be used in the NCSM. We will present results for flow parameters of $\alpha = 0.01\,{\rm fm}^4$, $\alpha = 0.04\,{\rm fm}^4$ (a typical value used in many-body calculations), and $\alpha = 0.20\,{\rm fm}^4$ corresponding to a very soft effective Hamiltonian $\widehat{H}_\alpha$.

The many-body problem for ^{4}He is then solved with the SRG transformed two-body Hamiltonian $\widehat{H}_\alpha$ using the shell model code Antoine [42]:

$$\widehat{H}_\alpha \big|\Psi_\alpha\rangle = E_\alpha \big|\Psi_\alpha\rangle \,. \tag{4}$$

The results for the ground state energy of ^{4}He and the two-body distributions in coordinate and momentum space discussed in this paper are well converged within the model space ($N_{\rm max} = 16$, oscillator parameter $\hbar\Omega = 36$MeV). The bare AV8' interaction ($\alpha = 0$) can however not be converged in this space and we use here the results obtained with the correlated Gaussian method [37, 40, 41].

All two-body information contained in the many-body states $\big|\Psi_\alpha\rangle$ can be expressed in terms of the two-body density matrix that is obtained by integrating over all coordinates besides the pair position and the relative coordinates of the pair. The two-body density as calculated in the NCSM is not translationally invariant due to the localization of the NCSM wave function in the origin of the coordinate system. However the translational invariant two-body density can be obtained from the two-body density in the laboratory system by a linear transformation as discussed in Appendix D. In the harmonic oscillator basis we express the two-body density matrix $\rho^\alpha_{qQ;q'Q'}$ with two-body basis states

$$\begin{aligned} \big|qQ\rangle &= \big|q\rangle \otimes \big|Q\rangle \\ &= \big|b_{\rm rel}; nlm, S\,M_S, T\,M_T\rangle \otimes \big|b_{\rm pair}; NLM\rangle \,. \end{aligned} \tag{5}$$

Here q summarizes the harmonic oscillator quantum numbers. nlm stand for the relative coordinates, $S\,M_S$ and $T\,M_T$ give the total spin and isospin of the pair, respectively, and Q summarizes the harmonic oscillator quantum numbers for the pair coordinate. The oscillator parameters for the relative and the pair motion are given by

$$b_{\rm rel} = \sqrt{2}\,b, \quad b_{\rm pair} = \sqrt{\frac{A}{2(A-2)}}\,b \,, \tag{6}$$

respectively.

A compact notation can be obtained by defining the two-body density operator, which acts in two-body space, as

$$\widehat{R}_\alpha = \sum_{qQ,q'Q'} \big|qQ\rangle\, \rho^\alpha_{qQ;q'Q'}\, \langle q'Q'\big| \,. \tag{7}$$

The expectation value of any 'bare' two-body operator $\widehat{B}$ can then simply evaluated as

$$B_\alpha := \langle\Psi_\alpha\big|\widehat{B}\big|\Psi_\alpha\rangle = {\rm Tr}_2\left(\widehat{R}_\alpha \widehat{B}\right) \,, \tag{8}$$

where Tr_2 denotes the trace in two-body space. If one evolves the observable $\widehat{B}$ in the same way as the Hamiltonian, namely $\widehat{B}_\alpha = \widehat{U}_\alpha^\dagger \widehat{B} \widehat{U}_\alpha$, the expectation value

$$\begin{aligned} \langle \Psi_\alpha | \widehat{B}_\alpha | \Psi_\alpha \rangle &= \langle \Psi_\alpha | \widehat{U}_\alpha^\dagger \widehat{B} \widehat{U}_\alpha | \Psi_\alpha \rangle \\ &= \langle \Psi_{\alpha=0} | \widehat{B} | \Psi_{\alpha=0} \rangle \end{aligned} \tag{9}$$

does not depend on α because $U_\alpha |\Psi_\alpha\rangle = |\Psi_{\alpha=0}\rangle$. However, as for the Hamiltonian, the evolved observable $\widehat{B}_\alpha$ is in general no longer a two-body operator and contains induced higher-body operators.

The two-body approximation consists in calculating

$$\widetilde{B}_\alpha := \mathrm{Tr}_2 \left(\widehat{R}_\alpha \widehat{B}_\alpha \right) = \mathrm{Tr}_2 \left(\widehat{U}_\alpha \widehat{R}_\alpha \widehat{U}_\alpha^\dagger \widehat{B} \right) , \tag{10}$$

where the two-body operator $\widehat{B}_\alpha$ is SRG transformed in two-body space. It should be noted that $\widehat{U}_\alpha$ acts only on the relative coordinate part of $\widehat{R}_\alpha$ or $\widehat{B}$ and leaves the center of mass motion of the pair unchanged.

If the two-body approximation was exact (for both the Hamiltonian $\widehat{H}$ and the observables $\widehat{B}$) $\widetilde{B}_\alpha$ would be α-independent. The remaining α dependence therefore indicates the size of the neglected contributions from the induced three- and higher-body terms.

With the many-body states $|\Psi_\alpha\rangle$ obtained in the NCSM various bare and SRG transformed two-body quantities will be studied in the following. With bare operators we can investigate how the properties of the eigenstates $|\Psi_\alpha\rangle$ change with increasing flow parameter. This will reflect the increasing 'softness' of the transformed Hamiltonian $\widehat{H}_\alpha$. On the other hand properties calculated with transformed operators should be independent from the flow parameter if the two-body approximation is justified. However one has to be careful when drawing conclusions about omitted higher-order terms in the transformed operators. In this paper the two-body approximation is employed both for the transformed Hamiltonian and for the transformed operators. Even if the two-body approximation is perfect for the transformed operators we would still expect a dependence on the flow parameter due to the two-body approximation for the transformation of the Hamiltonian.

It might be possible however that particular components of the wave function are less sensitive to higher-order terms in the transformed Hamiltonian and can be obtained reliably within the two-body approximation. This appears to be the case for the pairs with small pair momentum as will be discussed in Sec. III E.

III. RESULTS

A. Energies

In two-body approximation $\widehat{U}_\alpha$ is exactly unitary in two-body space, but in many-body space unitarity is only approximate. Therefore the energy eigenvalue E_α depends on α and this dependence can be taken as a measure for the induced three- and four-body interactions (see Eq. (3)) that are neglected when calculating the ^{4}He ground state energy in two-body approximation. As seen in Fig. 1 the total energy varies by about 10% indicating that the contribution of three- and four-body terms are small. In Fig. 1 we also show the individual contributions from the four S,T channels to the total ground state energy of ^{4}He. These can be calculated by using Eq. (10)

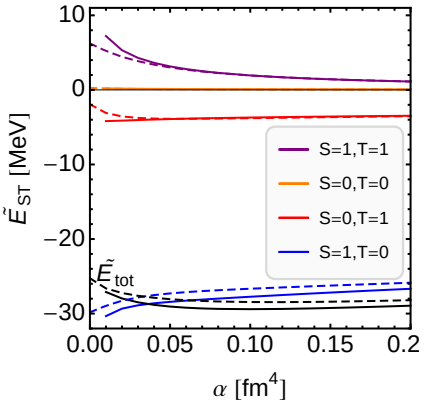

FIG. 1. (Color online) Contributions from the different S,T channels to the total energy of ^{4}He as a function of the flow parameter α for the AV8' interaction (solid) and the N3LO interaction (dashed). The total energy $\tilde{E}_{\mathrm{tot}}$ (black lines) includes the Coulomb energy.

$$\tilde{E}_{\alpha,ST} = \mathrm{Tr}_2 \left(\widehat{R}_\alpha [(\widehat{T}_{\mathrm{int}} + \widehat{V}_\alpha^{[2]}) \widehat{\Pi}_{ST} \otimes \widehat{1}] \right) , \tag{11}$$

where the operator $\widehat{\Pi}_{ST}$ projects on the spin-isospin channel S,T. The total energies for the AV8' and N3LO interactions are very similar (although the individual kinetic and potential contributions are quite different) and in both cases the dominant contribution to the binding energy is coming from $S,T = 1,0$ pairs with a large contribution from the tensor force. The $S,T = 0,1$ channel gives a much smaller attractive contribution whereas the $S,T = 1,1$ channel provides repulsion and the contribution from the $S,T = 0,0$ channel is negligible. With increasing flow parameter we observe a reduction of the attractive contribution of the $S,T = 1,0$ channel and the $S,T = 1,1$ contribution becomes less repulsive. These changes are related to changes in the occupation of the different S,T channels that will be discussed in Sec. III D.

B. Relative density distribution in coordinate space

The repulsive nature of the nuclear interaction is easily seen in the the relative density distribution $\rho_\alpha^{\mathrm{rel}}(r)$ that gives the probability to find a pair of nucleons at a distance r. It is calculated by replacing $\widehat{B}$ in Eq. (8) with the two-body operator

$$\widehat{\rho}^{\mathrm{rel}}(r) = \sum_{lmSM_ST M_T} |rlm, SM_S, TM_T\rangle\langle rlm, SM_S, TM_T| \otimes \widehat{1} , \tag{12}$$

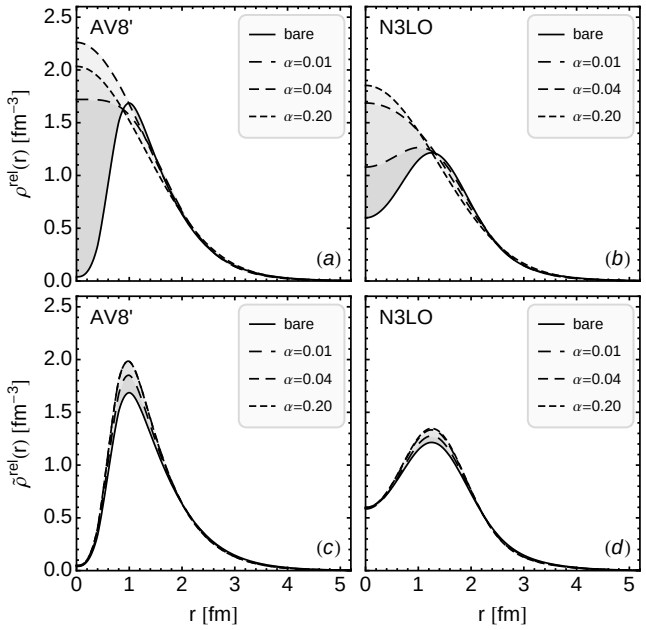

FIG. 2. AV8' (left) and N3LO (right) two-body densities in coordinate space calculated with bare (top) and SRG transformed density operators (bottom). α in units of fm^4. See also Fig. 1 in Ref. [43] for the AV8' two-body densities in the different S, T channels.

where we sum over all quantum numbers except the radial distance r.

The short-range correlations induced by the nuclear interaction are reflected in the relative density distributions $\rho^{\rm rel}_\alpha(r)$ shown in the upper part of Fig. 2. They are calculated with the eigenstates of the bare and SRG evolved Hamiltonians $\widehat{H}_\alpha$ according to Eq. (8). For the bare interactions the relative density distributions $\rho^{\rm rel}_{\alpha=0}(r)$ show the typical correlation hole at short distances. Due to the repulsive core of the interaction the probability to find a pair of nucleons at a distance r between their centers is depleted at distances below $r \approx 1$ fm. The chiral N3LO interaction is obviously not as repulsive as the AV8' interaction at short distances, as the correlation hole is less pronounced for the N3LO interaction.

One should keep in mind that the term 'correlation hole' is misleading as for $r \approx 0.5$ fm the nucleon densities are already strongly overlapping so that there is no hole in the baryonic matter density. On the contrary at short distances one encounters locally large baryonic matter densities and expects strongly polarized nucleons.

With increasing flow parameter α the correlation hole disappears more and more. Furthermore the density distributions calculated for the evolved AV8' and N3LO interactions become increasingly similar, cf. Fig. 2 (a), (b). For the largest flow parameter the relative density distribution is essentially of Gaussian shape — as would be expected for an uncorrelated mean-field wave function. Thus, the SRG transformation brings us from a highly correlated system to a simple shell model or mean-field like situation.

On the other hand the density distributions $\tilde{\rho}^{\rm rel}_\alpha(r)$ shown in the lower part of Fig. 2, which are obtained with the SRG transformed density operators according to Eq. (10), are all very similar to those obtained for the bare Hamiltonians $\widehat{H} \equiv \widehat{H}_{\alpha=0}$. Without employing the two-body approximation $\widehat{U}_\alpha$ would be unitary in four-body space and $\tilde{\rho}_\alpha$ would not depend on α. The remaining α dependence indicates that the induced three- and four-body terms are small but not completely negligible.

The probability densities obtained with both bare and transformed density operators are normalized to the number of pairs:

$$\int_0^\infty dr\, r^2\, \rho^{\rm rel}_\alpha(r) = \int_0^\infty dr\, r^2\, \tilde{\rho}^{\rm rel}_\alpha(r) = \frac{A(A-1)}{2} \qquad (13)$$

The spatial distributions shown in Fig. 2 may help our intuition but can not easily be related to experiment. Therefore momentum distributions and momentum correlations will be addressed in the following.

C. Relative momentum distributions

The relative momentum distribution, i.e., the probability $n^{\rm rel}_{\alpha,lST}(k)$ to find a nucleon pair with relative momentum k, relative orbital angular momentum l, spin S, and isospin T is obtained by replacing $\widehat{B}$ in Eq. (8) with the two-body operator

$$\widehat{n}^{\rm rel}_{lST}(k) = \sum_{mM_SM_T} \left|klm, SM_S, TM_T\right\rangle\!\left\langle klm, SM_S, TM_T\right| \otimes \widehat{1}\,, \qquad (14)$$

where $\left|klm, SM_S, TM_T\right\rangle$ denotes the spherical momentum space representation of the relative motion.

The relative momentum distributions for pairs with relative momentum k, irrespective of their orbital angular momentum l, spin S and isospin T, $n^{\rm rel}_\alpha(k) = \sum_{lST} n^{\rm rel}_{\alpha,lST}(k)$, and its SRG transformed partner $\tilde{n}^{\rm rel}_\alpha(k)$ are shown in Fig. 3 for the two interactions and different flow parameters. The short-range repulsive correlations, which manifest themselves in coordinate space as the correlation holes, show up as tails in the momentum distributions $n^{\rm rel}_\alpha(k)$ that reach out to large relative momenta k. Note however that the momentum distribution is not the Fourier transform of the diagonal two-body density in coordinate space.

Whereas the tail of the momentum distribution shows an exponential behavior at large relative momenta for the AV8' interaction, the N3LO relative momentum distribution reflects the momentum space regulator that cuts off high momenta beyond about 3.5 fm^{-1}. For both interactions short-range tensor correlations play an important role as will be discussed in more detail later. With increasing flow parameter α the high-momentum components are more and more reduced until the probability distribution of the relative momentum assumes a Gaussian shape for both evolved interactions, cf. Fig. 3 (a) and (b), corresponding to an uncorrelated wave function.

Fig. 3 (c) and (d) show that the density distributions $\tilde{n}^{\rm rel}_\alpha(k)$ obtained with the SRG transformed density operators are

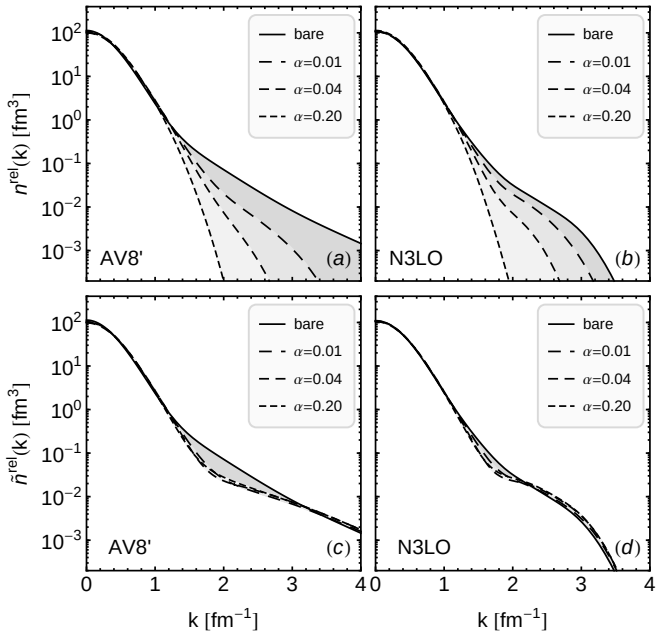

FIG. 3. AV8' (left) and N3LO (right) two-body densities in momentum-space calculated with bare (top) and SRG transformed density operators (bottom). α in units of fm^4. See also Fig. 2 in Ref. [43] for the AV8' two-body densities in the different S,T channels.

again all very similar to those obtained for the bare Hamiltonian, indicating that the induced three- and four-body terms are also small in momentum space. The most visible dependence on α occurs for the AV8' interaction around $k \approx 2\,\mathrm{fm}^{-1}$. This dependence is related to three-body correlations induced by the two-body tensor force to be discussed in the following subsection.

D. S,T relative momentum distributions

In order to get a deeper understanding of the nature of the correlations we separate the momentum distribution according to Eq. (14) into its parts $\tilde{n}^{\mathrm{rel}}_{\alpha,ST}(k) = \sum_l \tilde{n}^{\mathrm{rel}}_{\alpha,lST}(k)$ coming from the different S,T channels and display the results in Fig. 4. The first observation is that the $S,T = 1,0$ channel, in which the tensor force is strongest, shows only a weak α dependence. In contrast to that there is strong α dependence in the $S,T = 0,1$ channel for momenta around $2\,\mathrm{fm}^{-1}$ and also in the $S,T = 1,1$ channel. With increasing α strength moves from the odd $S,T = 1,1$ to the even $S,T = 0,1$ channel. This effect has been discussed in detail in Ref. [37]. In a simplified picture one may consider the situation of a localized $S,T = 0,1$ pair with a third nucleon of different flavor not too far away. Additional binding from the strong tensor force acting between the third nucleon and a nucleon of the pair can be obtained by flipping the spin of one nucleon in the $S,T = 0,1$ pair and thus converting with some probability the $S,T = 0,1$ pair into an $S,T = 1,1$ pair. It is energetically more favorable to break some $S,T = 0,1$ pairs and loose their binding if more binding from the tensor interaction with the third particle can be gained. These genuine three-body correlations are lost in two-body approximation and introduce an α-dependence. With increasing α the tensor part of the SRG transformed Hamiltonian $\widehat{H}_\alpha$ is weakened while the central part is strengthened. With the weakening of the tensor force the effect of the three-body correlations will be reduced. This explains the reduction of the number of $S,T = 1,1$ pairs with increasing α and the α-dependence of the $S,T = 0,1$ pairs at momenta around $2\,\mathrm{fm}^{-1}$ where the relative importance of the tensor force is most pronounced.

TABLE I. Number of pairs in the different (S,T) channels for the bare and SRG evolved AV8' and N3LO interactions.

$n^{\mathrm{pair}}_{\alpha,ST} = \tilde{n}^{\mathrm{pair}}_{\alpha,ST}$	(0,0)	(0,1)	(1,0)	(1,1)
AV8', bare	0.008	2.572	2.992	0.428
AV8', $\alpha = 0.01\,\mathrm{fm}^4$	0.008	2.708	2.992	0.292
AV8', $\alpha = 0.04\,\mathrm{fm}^4$	0.007	2.821	2.993	0.179
AV8', $\alpha = 0.20\,\mathrm{fm}^4$	0.005	2.925	2.995	0.075
N3LO, bare	0.009	2.710	2.991	0.290
N3LO, $\alpha = 0.01\,\mathrm{fm}^4$	0.007	2.745	2.992	0.255
N3LO, $\alpha = 0.04\,\mathrm{fm}^4$	0.006	2.817	2.994	0.183
N3LO, $\alpha = 0.20\,\mathrm{fm}^4$	0.004	2.921	2.995	0.079

This transfer of probability between the even $S,T = 0,1$ and the odd $S,T = 1,1$ channel can be seen in Table I where the number of pairs, $\tilde{n}^{\mathrm{pair}}_{\alpha,ST}$ given by the integrals over the momentum distributions, are listed as a function of α. With increasing flow parameter the occupation numbers approach the limit of the mean-field or independent particle model with 3 pairs in both even channels and 0 pairs in the odd channels. The number of pairs $n^{\mathrm{pair}}_{\alpha,ST}$ and $\tilde{n}^{\mathrm{pair}}_{\alpha,ST}$ obtained with bare and SRG transformed density operators are identical as $\widehat{U}_\alpha$ in two-body approximation does not connect different S,T channels.

The reshuffling of probability between the different spin-isospin channels also tells us that the omitted many-body terms in $\widehat{U}_\alpha$ and the transformed Hamiltonian $\widehat{H}_\alpha$ will have a non-trivial spin- and isospin-dependence.

E. Relative momentum distributions for $K = 0$ pairs

Up to now we have investigated relative momentum distributions for all pairs, indiscriminate of the pair momentum K. It has been found that the relative momentum distributions depend quite significantly on the pair momentum [23, 44]. In the context of this paper it is interesting to see how this is related to many-body correlations.

We might expect that back-to-back pairs with $\mathbf{K} \approx 0$ are less affected by many-body correlations than pairs with a large pair momentum $\mathbf{K}$. In a $K = 0$ pair with large relative momentum $\mathbf{k}$ both nucleons have large individual momenta. For pairs with large pair momentum $\mathbf{K}$ however there is a high probability that one of the nucleons has a momentum less than or close to Fermi momentum. We would therefore expect that

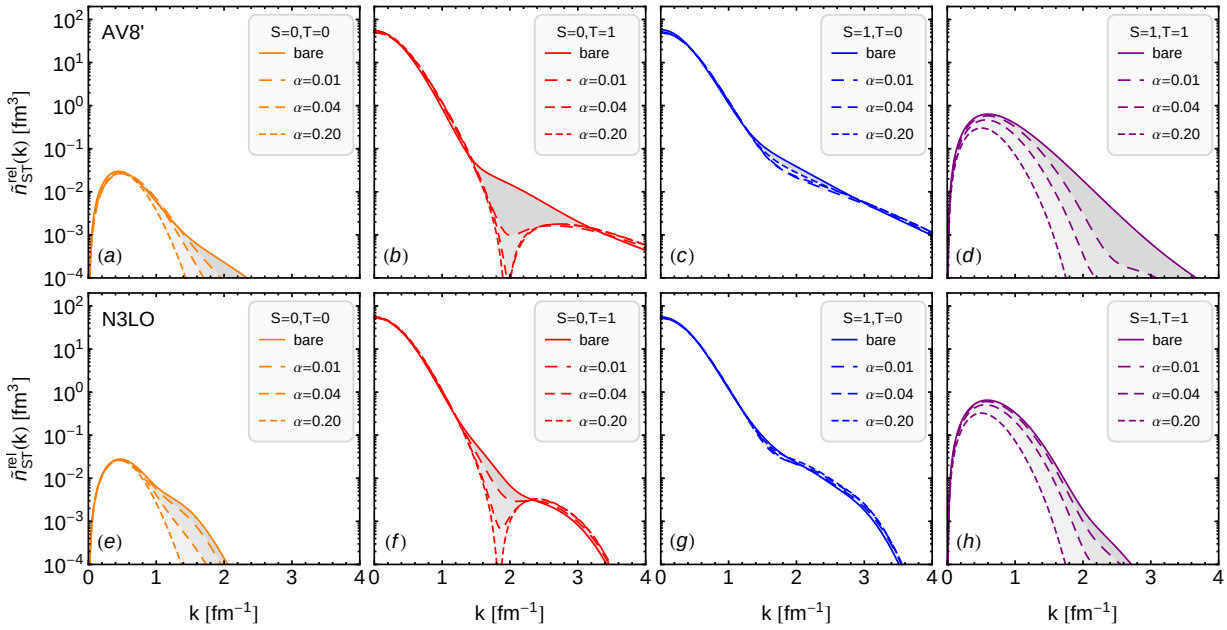

FIG. 4. (Color online) AV8' (top) and N3LO (bottom) relative momentum distributions in the different spin-isospin channels obtained with SRG transformed density operators. α in units of fm^4.

these nucleons are interacting more strongly with other nucleons and therefore are susceptible to many-body correlations.

In order to study this we investigate the more exclusive joint probability $\tilde{n}_{\alpha,ST}(k,K)$ to find a nucleon pair with spin S and isospin T at relative momentum k and total pair momentum K. It is calculated with the two-body operator

$$\widehat{n}_{lST}(k,K) = \sum_{mM_S M_T} \big|klm, SM_S, TM_T\rangle\langle klm, SM_S, TM_T\big| \otimes \sum_{LM} \big|KLM\rangle \left(\frac{A}{A-2}\right)^{3/2} \langle KLM\big|\,, \quad (15)$$

where $\big|KLM\rangle$ denotes the spherical momentum representation of the relative momentum of the pair with respect to the $A-2$ remaining nucleons. The factor $\left(\frac{A}{A-2}\right)^{3/2}$ originates from the transformation from Jacobi coordinates to the coordinates $\mathbf{k}$ and $\mathbf{K}$, see Sec. D. In this paper we consider only pair momentum $K = 0$ for which the sum over L, M reduces to $L = 0, M = 0$.

The momentum distributions $\tilde{n}_{\alpha,ST}(k, K = 0)$, obtained by summing $\tilde{n}_{\alpha,lST}(k, K = 0)$ over l, are displayed in Fig. 5. One sees that in all S, T channels the results are essentially independent on α. We can also observe that with increasing flow parameter α the momentum distributions $\tilde{n}_{\alpha,ST}(k)$, as shown in Fig. 4, become more and more similar to the momentum distributions $\tilde{n}_{\alpha,ST}(k, K = 0)$. This consistently tells us that for pairs with total momentum $K = 0$ many-body correlations are not very important, as anticipated in the discussion above. The $K = 0$ pairs are therefore the best candidates for experimental studies of short-range two-body correlations. Similar considerations can be found in Refs. [12, 23, 44].

We can also notice significant differences between the two even channels. In the $S, T = 0, 1$ channel the momentum distribution has a node at relative momenta of about 1.8 fm^{-1}. This is very different in the $S, T = 1, 0$ channel. Here the momentum distribution does not show a minimum and the number of pairs for relative momenta above about 1.5 fm^{-1} is significantly larger. This difference is due to short-range tensor correlations that only contribute in the $S, T = 1, 0$ channel. To illustrate this we show in Fig. 6 the momentum distributions in the $S, T = 1, 0$ channel decomposed into their contributions from different l for the AV8' and N3LO interactions. For the $K = 0$ distributions we do not have the results for the bare AV8' interaction and used the SRG transformed densities $\tilde{n}^{rel}_{lST}(k, K = 0)$ for $\alpha = 0.01$ fm^{-1} instead. Because of the very weak α dependence this should be equivalent to the exact result for the bare AV8' interaction. The distributions $\tilde{n}_{\alpha,lST}(k, K = 0)$ in this channel are of particular interest, because they show the dominant contribution from pairs with relative angular momentum $l = 2$ in the momentum region from 1.5 to almost 4 fm^{-1} for the AV8' and from 1.5 to about 2.5 fm^{-1} for the N3LO interaction. These D-wave pairs are directly reflecting the correlations induced by the tensor force. In the AV8' case the tensor correlations are present at all relative momenta and dominate over the $l = 0$ contribution for momenta above $k \approx 1.5$ fm^{-1}. For N3LO the regularization cuts them off at higher momenta so that they dominate only between $k \approx 1.5$ fm^{-1} and $k \approx 2.5$ fm^{-1}. It is important to note that the tensor correlations contribute also at low momenta. There is no natural scale in the tensor correlations that would allow to separate low and high momentum regions.

It is also interesting to compare the ^{4}He momentum distributions in the $S, T = 1, 0$ channel with those of the deuteron

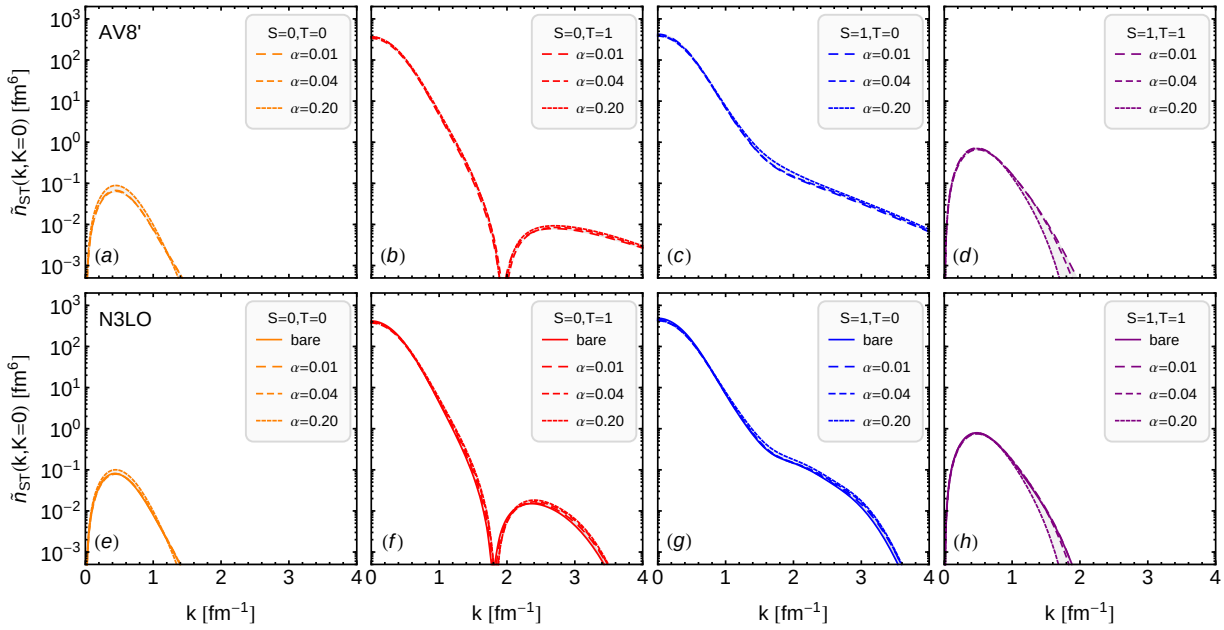

FIG. 5. (Color online) AV8' (top) and N3LO (bottom) relative momentum distributions for pairs with vanishing pair momentum $K = 0$ in the different spin-isospin channels obtained with SRG transformed density operators.

shown in Fig. 7. Whereas the momentum distributions in the low momentum region up to about $1.5\,\mathrm{fm}^{-1}$ are noticeably different, reflecting the differences in the long-range parts of the wave functions for the loosely bound deuteron and the strongly bound ^{4}He, the momentum distributions are almost indistinguishable for momenta above $1.5\,\mathrm{fm}^{-1}$. This is consistent with the observed universality of short-range correlations discussed in Ref. [37].

If we compare the momentum distributions for the $S, T = 1, 0$ pairs integrated over all pair momenta $\mathbf{K}$ as shown in Fig. 6 (a) and (b) with those for the corresponding $K = 0$ pairs we notice that the node for the S-wave pairs has vanished and that we find additional contributions from higher relative orbital angular momenta (G-wave pairs). This is consistent with our expectation that many-body correlations play a greater role for pairs with large pair momentum $\mathbf{K}$. This is further confirmed by a strong α dependence for these momentum distributions (not shown here). Alvioli *et al.* [44] found that the AV8' momentum distributions factorize in a relative and a pair distribution for pair momenta $\mathbf{K}$ up to about $1\,\mathrm{fm}^{-1}$, whereas for higher pair momenta the momentum distributions $n_{ST}(\mathbf{k}, \mathbf{K})$ no longer factorize and depend on the relative orientation of $\mathbf{k}$ and $\mathbf{K}$.

F. Relative probabilities for S, T pairs

The strength of two- and many-body correlations strongly depends on the relative momenta of the pairs. To highlight the relative importance of these correlations it is advantageous to look at the relative probabilities

$$\frac{n^{\mathrm{rel}}_{ST}(k)}{\sum_{ST} n^{\mathrm{rel}}_{ST}(k)}\,, \quad \frac{n_{ST}(k, K=0)}{\sum_{ST} n_{ST}(k, K=0)} \tag{16}$$

to find pairs in a given S, T channel as a function of relative momentum k. In Fig. 8 we show these relative probabilities for the bare AV8' and N3LO interactions. If we look at the relative probabilities for all pairs with relative momentum k it is obvious that the $S, T = 1, 1$ pairs contribute significantly, especially around $k \approx 1.5\,\mathrm{fm}^{-1}$. The total number of $S, T = 1, 1$ pairs is much smaller than the number of pairs in the even channels as shown in Tab. I, but in this mid-momentum region the number of pairs in the $S, T = 1, 1$ channel is comparable to those in the even channels. This is the region where many-body correlations have the largest effect. For small relative momenta the relative probabilities are dominated by the mean-field, for relative momenta above about $3\,\mathrm{fm}^{-1}$ in case of the AV8' and about $2.5\,\mathrm{fm}^{-1}$ in case of the N3LO interaction the relative probabilities are dominated by short-range correlations. This influence of many-body correlations is also related to a strong dependence on α. With increasing flow parameter α the relative probabilities for all pairs become more and more similar to the relative probabilities of the $K = 0$ pairs shown in Fig. 8 (c) and (d). As there is no significant α dependence for the $K = 0$ momentum distributions, the relative probabilities for the $K = 0$ pairs are independent from α as well and are therefore not sensitive to many-body correlations.

It is interesting to note that the relative probabilities for $K = 0$ the pairs are quite similar for the AV8' and N3LO interactions, even for very large relative momenta, whereas the absolute values of the momentum distributions are very dif-

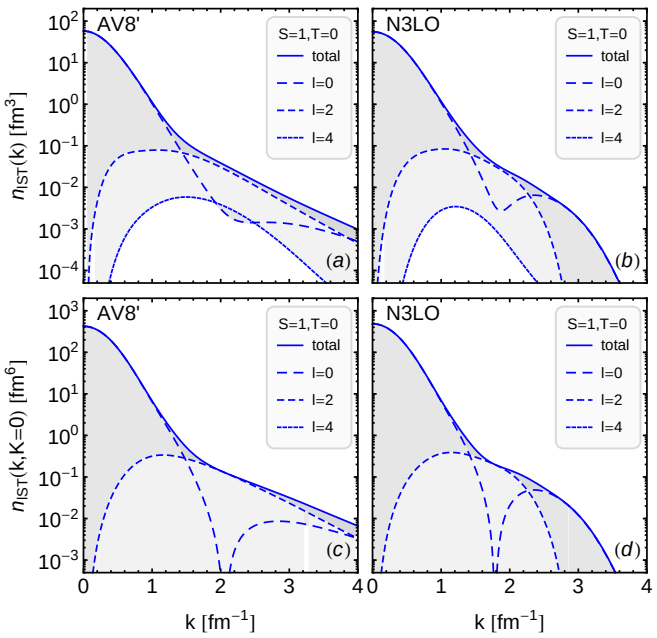

FIG. 6. (Color online) Momentum distributions for the bare AV8' and N3LO interactions in the $S,T = 1,0$ channel decomposed into contributions from pairs with relative orbital angular momentum $l = 0,2,4$. For all pairs (top) and for pairs with vanishing pair momentum (bottom).

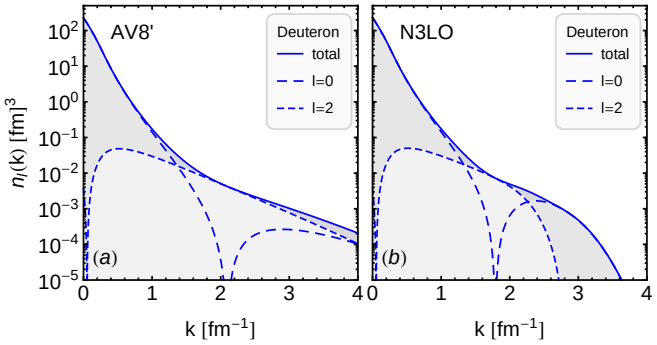

FIG. 7. (Color online) Total, $l = 0$ and $l = 2$ momentum distributions in the deuteron ($S,T = 1,0$) for the AV8' and the N3LO interactions.

ferent. Differences in the relative probabilities between AV8' and N3LO reflect differences in the relative importance of tensor correlations for the two interactions due to differences in the regularization of the tensor force.

G. Relative probabilities for pn and pp pairs

In an experiment one measures protons and neutrons and not S,T pairs. Therefore we define the operator in two-body space that measures the probability to find a pair of two protons (pp: $M_T = 1$) or a proton-neutron pair ($pn+np$: $M_T = 0$)

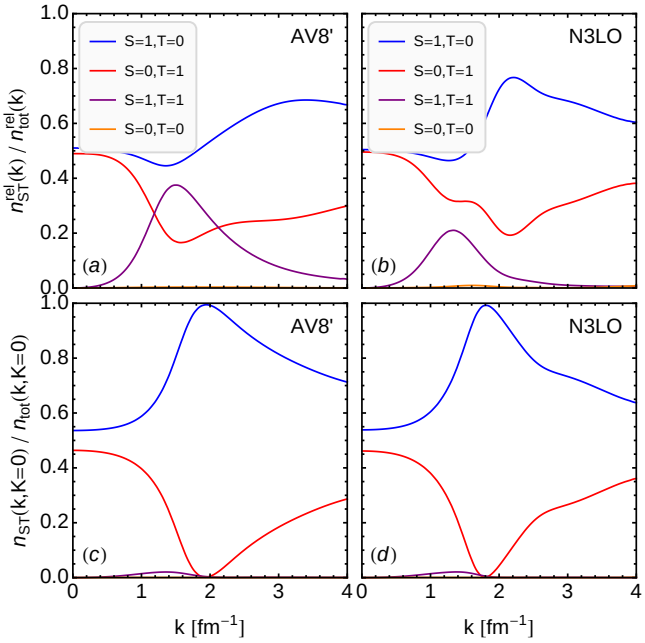

FIG. 8. (Color online) Relative probability to find pairs in the different spin-isospin channels as a function of relative momentum. For all pairs (top) or only for pairs with pair momentum $K = 0$ (bottom).

at relative momentum k and pair momentum K as

$$\widehat{n}_{M_T}(k,K) = \sum_{lm,SM_S,T} \left|klm,SM_S,TM_T\right\rangle\left\langle klm,SM_S,TM_T\right| \otimes \sum_{LM} \left|KLM\right\rangle \left(\frac{A}{A-2}\right)^{3/2} \left\langle KLM\right| . \quad (17)$$

In the case of ^{4}He one $T = 0$ pair corresponds to one pn-pair, and one $T = 1$ pair to $\frac{1}{3}$ of a pp, $\frac{1}{3}$ of a nn and $\frac{1}{3}$ of a pn pair.

The corresponding relative probabilities for $K = 0$ pairs

$$\frac{n_{M_T}(k,K=0)}{\sum_{M_T} n_{M_T}(k,K=0)} \quad (18)$$

are shown in Fig. 9. The first observation is that the relative probabilities are rather similar for the AV8' and N3LO interactions. At low momenta both show a ratio close to $\frac{1}{4}$ to find pp versus pn pairs. This is to be expected because an uncorrelated system of two protons and two neutrons can form one pp-pair, one nn-pair but four pn-pairs.

Around $k \approx 1.8\,\mathrm{fm}^{-1}$ the minimum in the $S,T = 0,1$ channel (see Fig. 5) together with the $l = 2$ contribution from the tensor interaction in the $S,T = 1,0$ channel (see Fig. 6) enhances the relative probability to find a pn pair to almost 100%. This dominance of pn pairs has been observed in exclusive two-nucleon knockout experiments [13, 15]. Recently the pn to pp ratio has been measured for relative momenta k from $2.5\,\mathrm{fm}^{-1}$ up to almost $4\,\mathrm{fm}^{-1}$ [17] showing an increase in the pp/pn ratio. Within the experimental uncertainties the

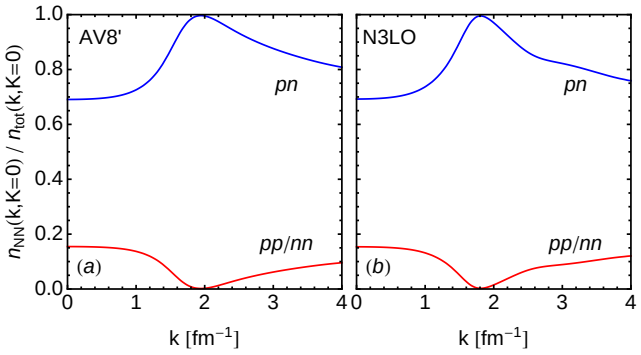

FIG. 9. (Color online) Relative probability to find pn or pp pairs with pair momentum $K = 0$ as a function of relative momentum.

data agree with our results for both AV8' and N3LO interactions.

IV. SUMMARY AND CONCLUSIONS

In this paper we applied the SRG formalism for the calculation of relative density and momentum distributions of ^{4}He. The ^{4}He ground state wave functions are calculated in the NCSM with the SRG evolved AV8' and N3LO interactions in two-body approximation. Two-body densities in coordinate and momentum space calculated with the unevolved density operators illustrate how short-range correlations are eliminated by the SRG evolution. With increasing flow parameter α the interaction gets 'softer' and the wave functions become essentially uncorrelated mean-field wave functions without correlation holes and high-momentum components. The short-range or high-momentum information can be recovered by calculating two-body densities with the SRG evolved density operators, again in two-body approximation. Using these effective density operators we see a dependence of the two-body densities on the flow parameter α. This α dependence is due to missing contributions from three- and four-body terms in the effective operators, that are omitted in the two-body approximation. We find that not all components of the two-body density are equally affected by many-body correlations. The momentum distributions for pairs with pair momentum $K = 0$ show only a very weak α dependence and therefore provide direct access to two-body short-range correlations. The momentum distributions integrated over all pair momenta on the other hand have a sizeable α dependence. This α dependence is particularly strong in the $S, T = 0, 1$ and $S, T = 1, 1$ channels for momenta around 1.5 fm^{-1}. We identified three-body correlations induced by the strong tensor force as the main contributor to these many-body correlations.

Our results for the AV8' momentum distributions agree with previous results [22–24, 44] using variational Monte-Carlo and few-body approaches. We confirm the important role of tensor correlations that explain the experimentally observed dominance of pn over pp pairs in exclusive two-nucleon knock-out with large momentum transfer. We also show that the chiral N3LO interaction provides very similar results for the momentum distributions at least up to relative momenta of $2.5 - 3.0$ fm^{-1}. This includes the role of tensor correlations that are very similar for both interactions. At larger relative momenta the N3LO momentum distributions fall off much faster than the AV8' momentum distributions as would be expected from the relatively soft cutoff employed in the regularization of the N3LO interaction. These differences are however mostly hidden in the ratios of pn versus pp pairs as a function of relative momenta as investigated in two-nucleon knockout experiments. Recently new chiral interactions with different regularization schemes have been proposed [45, 46]. It will be interesting to see how these affect the short-range behavior and momentum distributions.

In this paper we investigated the ^{4}He nucleus as it allowed us to compare SRG evolved with bare interactions. SRG evolved soft Hamiltonians however will allow us to study heavier nuclei in the p-shell using the NCSM. One interesting question is the isospin dependence of the short-range correlations [47, 48] in asymmetric nuclei. Neutron halos or skins might be a useful laboratory for the study of neutron matter. The present study also did not include three-body forces. Wiringa *et al.* [24] find only small differences in the proton momentum distributions obtained with AV18 alone and AV18 together with an UX three-body interaction. We would expect that three-body interactions would not significantly change the short-range two-body correlations in the $K = 0$ pairs, they may however have a significant effect on the many-body correlations and therefore change the results for the momentum distributions integrated over all pair momenta.

Appendix A: Talmi-Moshinsky transformation

For an orthogonal transformation of the coordinates $(\mathbf{x}_1, \mathbf{x}_2)$ into $(\mathbf{X}, \mathbf{x})$ with the mass ratio $d = A_1/A_2$

$$\begin{pmatrix} \mathbf{X} \\ \mathbf{x} \end{pmatrix} = \begin{pmatrix} \sqrt{\frac{d}{1+d}} & \sqrt{\frac{1}{1+d}} \\ \sqrt{\frac{1}{1+d}} & -\sqrt{\frac{d}{1+d}} \end{pmatrix} \begin{pmatrix} \mathbf{x}_1 \\ \mathbf{x}_2 \end{pmatrix} \tag{A1}$$

the product of harmonic oscillator wave functions in coordinates $\mathbf{x}_1$ and $\mathbf{x}_2$ can be expressed with the Talmi-Moshinsky brackets $\langle NL, nl : \Lambda |\, n_1 l_1, n_2 l_2 : \Lambda \rangle_d$ in the new coordinates as:

$$\begin{aligned} \sum_{m_1 m_2} \left\langle \begin{matrix} l_1 & l_2 \\ m_1 & m_2 \end{matrix} \middle| \begin{matrix} \Lambda \\ \lambda \end{matrix} \right\rangle \varphi^b_{n_1 l_1 m_1}(\mathbf{x}_1) \varphi^b_{n_2 l_2 m_2}(\mathbf{x}_2) = \\ \sum_{NL,nl} \langle NL, nl : \Lambda |\, n_1 l_1, n_2 l_2 : \Lambda \rangle_d \\ \times \sum_{Mm} \left\langle \begin{matrix} L & l \\ M & m \end{matrix} \middle| \begin{matrix} \Lambda \\ \lambda \end{matrix} \right\rangle \varphi^b_{NLM}(\mathbf{X}) \varphi^b_{nlm}(\mathbf{x}) \end{aligned} \tag{A2}$$

All harmonic oscillator wave functions have the same oscillator parameter b. See Ref. [49] for further properties.

Appendix B: Jacobi coordinates

The wave function and two-body densities in the intrinsic system will be expressed in Jacobi coordinates. We follow [50] and use mass-scaled Jacobi coordinates that fulfill the orthogonality condition (A1):

$$\boldsymbol{\xi}_0 = \sqrt{\frac{1}{A}}\,[\mathbf{x}_1 + \ldots + \mathbf{x}_A] \tag{B1}$$

$$\boldsymbol{\xi}_1 = \sqrt{\frac{1}{2}}\,[\mathbf{x}_1 - \mathbf{x}_2] \tag{B2}$$

$$\boldsymbol{\xi}_2 = \sqrt{\frac{2}{3}}\left[\frac{1}{2}(\mathbf{x}_1 + \mathbf{x}_2) - \mathbf{x}_3\right] \tag{B3}$$

$$\vdots$$

$$\boldsymbol{\xi}_{A-1} = \sqrt{\frac{A-1}{A}}\left[\frac{1}{A-1}(\mathbf{x}_1 + \ldots + \mathbf{x}_{A-1}) - \mathbf{x}_A\right] \tag{B4}$$

The transformation from the coordinates $(\mathbf{x}_1, \ldots, \mathbf{x}_A)$ to $(\boldsymbol{\xi}_0, \ldots, \boldsymbol{\xi}_{A-1})$ is orthogonal. Translational invariant one-body densities can be expressed in these Jacobi coordinates. For the two-body densities we prefer however a different set of Jacobi coordinates where we have the distance between the nucleons and the distance of the center of mass of the pair with respect to the rest of the nucleus as coordinates. This can be achieved by an additional orthogonal transformation from the coordinates $(\boldsymbol{\xi}_{A-2}, \boldsymbol{\xi}_{A-1})$ into the coordinates $(\boldsymbol{\eta}, \boldsymbol{\vartheta})$

$$\boldsymbol{\eta} = \sqrt{\frac{2(A-2)}{A}} \times \left[\frac{1}{A-2}(\mathbf{x}_1 + \ldots + \mathbf{x}_{A-2}) - \frac{1}{2}(\mathbf{x}_{A-1} + \mathbf{x}_A)\right], \tag{B5}$$

$$\boldsymbol{\vartheta} = \sqrt{\frac{1}{2}}[\mathbf{x}_{A-1} - \mathbf{x}_A]\,. \tag{B6}$$

Appendix C: Two-body densities in the laboratory system

In the NCSM the wave function is expanded in a harmonic oscillator single-particle basis with oscillator parameter b

$$\big|q\big\rangle = \big|b; nlm, m_s, m_t\big\rangle\,. \tag{C1}$$

The NCSM uses second quantization techniques and the two-body density in the harmonic oscillator basis can be expressed as

$$\rho^{\rm lab}_{q_1' q_2'; q_1 q_2} = \langle\Psi\big|\widehat{a}^\dagger_{q_1}\widehat{a}^\dagger_{q_2}\widehat{a}_{q_2'}\widehat{a}_{q_1'}\big|\Psi\rangle\,. \tag{C2}$$

For the discussion of two-body correlations it is natural to transform from single-particle to pair coordinates. In the laboratory system we define relative and pair coordinates as

$$\mathbf{r} = \mathbf{x}_1 - \mathbf{x}_2, \quad \mathbf{R} = \frac{1}{2}(\mathbf{x}_1 + \mathbf{x}_2)\,, \tag{C3}$$

and the conjugate coordinates in momentum space as

$$\mathbf{k} = \frac{1}{2}(\mathbf{p}_1 - \mathbf{p}_2), \quad \mathbf{K} = \mathbf{p}_1 + \mathbf{p}_2\,. \tag{C4}$$

These coordinates differ from the ones in (A1) by factors of $\sqrt{2}$ and $1/\sqrt{2}$ so that the oscillator parameters for the relative and the pair motion have to changed to $b_{\rm rel} = \sqrt{2}\,b$ and $b_{\rm pair} = \frac{1}{\sqrt{2}}\,b$ respectively. Using (A2) and coupling orbital angular momenta, spins and isospins the two-body density (C2) can be transformed into $\rho^{\rm lab}_{qQ;q'Q'}$.

Using this new basis

$$\big|qQ\big\rangle = \big|b_{\rm rel}; nlmS\,M_S\,T\,M_T\big\rangle \otimes \big|b_{\rm pair}; NLM\big\rangle \tag{C5}$$

we can define the density operator in two-body space as

$$\widehat{R}^{\rm lab} = \sum_{qQ;q'Q'} \big|qQ\big\rangle\rho^{\rm lab}_{qQ;q'Q'}\big\langle q'Q'\big|\,. \tag{C6}$$

$\widehat{R}^{\rm lab}$ allows to easily express the two-body density in coordinate space as a function of relative distance $\mathbf{r}$ and pair position $\mathbf{R}$

$$\rho^{\rm lab}(\mathbf{r}, \mathbf{R}) = {\rm Tr}_2\left(\widehat{R}^{\rm lab}\,\big|\mathbf{r}; \mathbf{R}\big\rangle\big\langle\mathbf{r}; \mathbf{R}\big|\right)\,, \tag{C7}$$

or as function of relative momentum $\mathbf{k}$ and pair momentum $\mathbf{K}$

$$n^{\rm lab}(\mathbf{k}, \mathbf{K}) = {\rm Tr}_2\left(\widehat{R}^{\rm lab}\,\big|\mathbf{k}; \mathbf{K}\big\rangle\big\langle\mathbf{k}; \mathbf{K}\big|\right)\,. \tag{C8}$$

This can be trivially extended to calculate off-diagonal densities or densities for pairs of a given spin and isospin.

These densities can also be expressed as

$$\rho^{\rm lab}(\mathbf{r}, \mathbf{R}) = \sum_{i<j}\langle\Psi\big|\delta^3(\widehat{\mathbf{x}}_i - \widehat{\mathbf{x}}_j - \mathbf{r})\delta^3(\frac{1}{2}(\widehat{\mathbf{x}}_i + \widehat{\mathbf{x}}_j) - \mathbf{R})\big|\Psi\rangle \tag{C9}$$

and can be obtained from the wave functions by integrating out $A-2$ coordinates (we have omitted spin- and isospin indices for brevity)

$$\rho^{\rm lab}(\mathbf{r}, \mathbf{R}) = \frac{A(A-1)}{2}\int d^3x_1 \cdots d^3x_{A-2}\, \Psi(\mathbf{x}_1, \ldots, \mathbf{x}_{A-2}, \mathbf{R} + \tfrac{1}{2}\mathbf{r}, \mathbf{R} - \tfrac{1}{2}\mathbf{r})^* \times \Psi(\mathbf{x}_1, \ldots, \mathbf{x}_{A-2}, \mathbf{R} + \tfrac{1}{2}\mathbf{r}, \mathbf{R} - \tfrac{1}{2}\mathbf{r})\,, \tag{C10}$$

where we have used the antisymmetry of the wave function.

Appendix D: Two-body densities in the intrinsic system

The two-body density $\rho^{\rm lab}_{qQ;q'Q'}$ is calculated in the harmonic oscillator basis of the NCSM localized at the origin of the coordinate system and is therefore not translationally invariant. However the wave function in the NCSM factorizes into an intrinsic wave function only depending on relative coordinates

and the total center-of-mass wave function in the ground state of the harmonic oscillator [51]

$$\Psi(\mathbf{x}_1,\ldots,\mathbf{x}_A) = \Psi_{\rm int}(\boldsymbol{\xi}_1,\ldots,\boldsymbol{\xi}_{A-3},\boldsymbol{\eta},\boldsymbol{\vartheta})\varphi^b_{000}(\boldsymbol{\xi}_0)\,. \tag{D1}$$

This allows us to relate the two-body density in the laboratory system $\rho^{\rm lab}_{qQ;q'Q'}$ with the two-body density in the intrinsic system. The derivation is lengthy but straightforward and follows the derivation of the translational invariant one-body density in Ref. [50].

One starts with the two-body density in the laboratory system as given from the wave functions written in the coordinates $\mathbf{x}_1,\ldots,\mathbf{x}_{A-2},\mathbf{X}_2 = \frac{1}{\sqrt{2}}(\mathbf{x}_{A-1}+\mathbf{x}_A)$ and $\boldsymbol{\vartheta} = \frac{1}{\sqrt{2}}(\mathbf{x}_{A-1}-\mathbf{x}_A)$:

$$\begin{aligned}\rho^{\rm lab}_{q',N'_2L'_2M'_2;qN_2L_2M_2} = \frac{A(A-1)}{2}\int d^3x_1\cdots d^3x_{A-2}\,d^3X_2\,d^3\vartheta\int d^3x'_1\cdots d^3x'_{A-2}\,d^3X'_2\,d^3\vartheta'\\ \times\Psi(\mathbf{x}_1,\ldots,\mathbf{x}_{A-2},\mathbf{X}_2,\boldsymbol{\vartheta})^*\delta^3(\mathbf{x}_1-\mathbf{x}'_1)\cdots\delta^3(\mathbf{x}_{A-2}-\mathbf{x}'_{A-2})\Psi(\mathbf{x}'_1,\ldots,\mathbf{x}'_{A-2},\mathbf{X}'_2,\boldsymbol{\vartheta}')\\ \times\varphi_{N'_2L'_2M'_2}(\mathbf{X}'_2)^*\,\varphi_{N_2L_2M_2}(\mathbf{X}_2)\,\varphi_{q'}(\boldsymbol{\vartheta}')^*\,\varphi_q(\boldsymbol{\vartheta})\end{aligned} \tag{D2}$$

We now perform an orthogonal coordinate transformation from $(\mathbf{x}_1,\ldots,\mathbf{x}_{A-2},\mathbf{X}_2)$ to $(\mathbf{X}_{A-2},\boldsymbol{\xi}_1,\ldots,\boldsymbol{\xi}_{A-3})$ and correspondingly for the primed coordinates. Next one uses the properties of the delta function to obtain delta functions in the Jacobi coordinates $\boldsymbol{\xi}_k$ and in $\mathbf{X}_{A-2} = \frac{1}{\sqrt{A-2}}\sum_{i=1}^{A-2}\mathbf{x}_i$. The delta function in $\mathbf{X}_{A-2}$ is expanded in the harmonic oscillator basis

$$\delta^3(\mathbf{X}_{A-2}-\mathbf{X}'_{A-2}) = \sum_{N_{A-2}L_{A-2}M_{A-2}}\varphi_{N_{A-2}L_{A-2}M_{A-2}}(\mathbf{X}_{A-2})\,\varphi_{N_{A-2}L_{A-2}M_{A-2}}(\mathbf{X}'_{A-2})^*\,. \tag{D3}$$

In the next step a second orthogonal coordinate transformation from $(\mathbf{X}_{A-2},\mathbf{X}_2)$ to $(\boldsymbol{\xi}_0,\boldsymbol{\eta})$ is performed employing the Talmi-Moshinsky transformation for the harmonic oscillator wave functions, rewriting products $\varphi_{N_{A-2}L_{A-2}M_{A-2}}(\mathbf{X}_{A-2})\varphi_{N_2L_2M_2}(\mathbf{X}_2)$ with linear combinations of products $\varphi_{N_{\rm cm}L_{\rm cm}M_{\rm cm}}(\boldsymbol{\xi}_0)\varphi_{NLM}(\boldsymbol{\eta})$.

If one uses (D1) one can now integrate over $\boldsymbol{\xi}_0$ and $\boldsymbol{\xi}'_0$ to express the density matrix in the laboratory system with the intrinsic wave functions so that the density matrix in the laboratory system can be related to the density matrix in the intrinsic system:

$$\begin{aligned}\rho_{q',N'L'M';qNLM} = \frac{A(A-1)}{2}\int d^3\xi_1\cdots d^3\xi_{A-3}\,d^3\eta\,d^3\eta'\,d^3\vartheta\,d^3\vartheta'\\ \times\Psi_{\rm int}(\boldsymbol{\xi}_1,\ldots,\boldsymbol{\xi}_{A-3},\boldsymbol{\eta},\boldsymbol{\vartheta})^*\Psi_{\rm int}(\boldsymbol{\xi}_1,\ldots,\boldsymbol{\xi}_{A-3},\boldsymbol{\eta}',\boldsymbol{\vartheta}')\,\varphi_{N'L'M'}(\boldsymbol{\eta}')^*\,\varphi_{NLM}(\boldsymbol{\eta})\,\varphi_{q'}(\boldsymbol{\vartheta}')^*\,\varphi_q(\boldsymbol{\vartheta})\end{aligned} \tag{D4}$$

In this paper we only discuss scalar densities in the pair coordinates (integrating over all pair momenta $\mathbf{K}$ or $K=0$). Then $L=L'$ and $M=M'$ and we can use the completeness relations for the Clebsch-Gordan coefficients to obtain the relation between the density matrices in the laboratory (D2) and the intrinsic system (D4)

$$\sum_{M_2}\rho^{\rm lab}_{q'N'_2L_2M_2;qN_2L_2M_2} = \sum_{NN'L}M^{(0)}_{N'_2L_2,N_2L_2;N'L,NL}\sum_M\rho_{q'N'LM;qNLM}\,. \tag{D5}$$

with the transformation matrix $M^{(0)}$

$$M^{(0)}_{N'_2L_2,N_2L_2;N'L,NL} = \sum_{N_{A-2}L_{A-2}}\langle 00,NL:L|\,N_{A-2}L_{A-2},N_2L_2:L\rangle_{(A-2)/2}\,\langle 00,N'L:L\big|\,N_{A-2}L_{A-2},N'_2L_2:L\rangle_{(A-2)/2} \tag{D6}$$

given by the Talmi-Moshinsky brackets with the mass ratio $d=\frac{A-2}{2}$. This reflects the distribution of the oscillator quanta among the nucleon pair and the $A-2$ remaining nucleons. The translationally invariant two-body density averaged over the orientations of the pair momenta $\sum_M\rho_{q'N'LM;qNLM}$ is then obtained from the two-body density matrix in the laboratory system by inverting Eq. (D5).

The two-body density in the Jacobi coordinates $\boldsymbol{\eta}$ and $\boldsymbol{\vartheta}$ is given by

$$\rho^{\rm jac}(\boldsymbol{\vartheta},\boldsymbol{\eta}) = \sum_{qNLM,q'N'L'M'}\rho_{q'N'L'M';qNLM}\,\varphi^b_{NLM}(\boldsymbol{\eta})^*\,\varphi^b_{N'L'M'}(\boldsymbol{\eta})\,\varphi^b_q(\boldsymbol{\vartheta})^*\,\varphi^b_{q'}(\boldsymbol{\vartheta}) \tag{D7}$$

The mass-scaled Jacobi coordinates have technical advantages, however we prefer to express the two-body densities in the more intuitive coordinates

$$\mathbf{r} = \mathbf{x}_{A-1}-\mathbf{x}_A,\quad \mathbf{R} = \frac{1}{2}(\mathbf{x}_{A-1}+\mathbf{x}_A) - \frac{1}{A-2}(\mathbf{x}_1+\ldots+\mathbf{x}_{A-2}) \tag{D8}$$

that are related to the Jacobi coordinates by

$$\mathbf{r} = \sqrt{2}\,\boldsymbol{\vartheta}, \quad \mathbf{R} = -\sqrt{\frac{A}{2(A-2)}}\,\boldsymbol{\eta}\,. \tag{D9}$$

The conjugate variables to $\mathbf{r}$ and $\mathbf{R}$ are the relative momentum of the nucleons in the pair $\mathbf{k}$ and the relative momentum of the pair with respect to the rest of the nucleus $\mathbf{K}$ (in the center-of-mass system this is the same as the momentum of the pair).

$$\mathbf{k} = \frac{1}{2}(\mathbf{p}_{A-1} - \mathbf{p}_A), \quad \mathbf{K} = \frac{A-2}{A}(\mathbf{p}_{A-1} + \mathbf{p}_A) - \frac{2}{A}(\mathbf{p}_1 + \ldots + \mathbf{p}_{A-2}) \tag{D10}$$

The two-body density in these coordinates is then

$$\begin{aligned}\rho(\mathbf{r},\mathbf{R}) &= \left(\frac{A-2}{A}\right)^{3/2} \rho^{\mathrm{jac}}\left(\frac{1}{\sqrt{2}}\mathbf{r}, -\sqrt{\frac{2(A-2)}{A}}\mathbf{R}\right) \\ &= \left(\frac{A-2}{A}\right)^{3/2} \sum_{qNLM,q'N'L'M'} \rho_{q'N'L'M';qNLM}\, \varphi^{b_{\mathrm{pair}}}_{NLM}(\mathbf{R})^*\, \varphi^{b_{\mathrm{pair}}}_{N'L'M'}(\mathbf{R})\, \varphi^{b_{\mathrm{rel}}}_{q}(\mathbf{r})^*\, \varphi^{b_{\mathrm{rel}}}_{q'}(\mathbf{r})\end{aligned} \tag{D11}$$

Note that the oscillator parameter for the pair motion $b_{\mathrm{pair}} = \sqrt{\frac{A}{2(A-2)}}\,b$ is different than in the laboratory system, whereas the oscillator parameter $b_{\mathrm{rel}} = \sqrt{2}\,b$ is the same. The factor $\left(\frac{A-2}{A}\right)^{3/2}$ is the Jacobian of the nonorthogonal transformation from the coordinates $\boldsymbol{\vartheta}$ and $\boldsymbol{\eta}$ to $\mathbf{r}$ and $\mathbf{R}$ in (D9).

As in the laboratory system a convenient notation is obtained by defining the density operator in two-body space

$$\widehat{R} = \sum_{qQ;q'Q'} |qQ\rangle \rho_{qQ;q'Q'} \langle q'Q'| \tag{D12}$$

with

$$|qQ\rangle = |b_{\mathrm{rel}}; nlmS\,M_S\,T\,M_T\rangle \otimes |b_{\mathrm{pair}}; NLM\rangle\,. \tag{D13}$$

The two-body densities in coordinate space can then be expressed as

$$\rho(\mathbf{r},\mathbf{R}) = \mathrm{Tr}_2\left(\widehat{R}\,|\mathbf{r};\mathbf{R}\rangle \left(\frac{A-2}{A}\right)^{3/2} \langle \mathbf{r};\mathbf{R}|\right) \tag{D14}$$

and in momentum space as

$$n(\mathbf{k},\mathbf{K}) = \mathrm{Tr}_2\left(\widehat{R}\,|\mathbf{k};\mathbf{K}\rangle \left(\frac{A}{A-2}\right)^{3/2} \langle \mathbf{k};\mathbf{K}|\right)\,. \tag{D15}$$

ACKNOWLEDGMENTS

We acknowledge support by the ExtreMe Matter Institute EMMI in the framework of the Helmholtz Alliance HA216/EMMI and by JSPS KAKENHI Grant Number 25800121.

[1] R. B. Wiringa, V. G. J. Stoks, and R. Schiavilla, Phys. Rev. C **51**, 38 (1995).
[2] R. Machleidt, Phys. Rev. C **63**, 024001 (2001).
[3] D. R. Entem and R. Machleidt, Phys. Rev. C **68**, 041001 (2003).
[4] E. Epelbaum, W. Glöckle, and U.-G. Meißner, Nucl. Phys. A **747**, 362 (2005).
[5] O. Benhar, A. Fabrocini, S. Fantoni, and I. Sick, Nucl. Phys. A **579**, 493 (1994).
[6] V. R. Pandharipande, I. Sick, and P. K. A. d. Huberts, Rev. Mod. Phys. **69**, 981 (1997).
[7] H. Müther and A. Polls, Prog. Part. Nucl. Phys. **45**, 243 (2000).
[8] T. Neff and H. Feldmeier, Nucl. Phys. A **713**, 311 (2003).
[9] W. Dickhoff and C. Barbieri, Prog. Part. Nucl. Phys. **52**, 377 (2004).
[10] A. Rios, A. Polls, and W. H. Dickhoff, Phys. Rev. C **79**, 064308 (2009).
[11] L. Frankfurt, M. Sargsian, and M. Strikman, Int. J. Mod. Phys. A **23**, 2991 (2008).
[12] J. Arrington, D. Higinbotham, G. Rosner, and M. Sargsian, Prog. Part. Nucl. Phys. **67**, 898 (2012).
[13] A. Tang, J. W. Watson, J. Aclander, J. Alster, G. Asryan, Y. Averichev, D. Barton, V. Baturin, N. Bukhtoyarova, A. Carroll, S. Gushue, S. Heppelmann, A. Leksanov, Y. Makdisi, A. Malki, E. Minina, I. Navon, H. Nicholson, A. Ogawa, Y. Panebratsev, E. Piasetzky, A. Schetkovsky, S. Shimanskiy, and D. Zhalov, Phys. Rev. Lett. **90**, 042301 (2003).
[14] R. Shneor *et al.* (Jefferson Lab Hall A Collaboration), Phys. Rev. Lett. **99**, 072501 (2007).
[15] R. Subedi, R. Shneor, P. Monaghan, B. D. Anderson, K. Aniol, J. Annand, J. Arrington, H. Benaoum, F. Benmokhtar, W. Boeglin, J.-P. Chen, S. Choi, E. Cisbani, B. Craver, S. Frullani, F. Garibaldi, S. Gilad, R. Gilman, O. Glamazdin, J.-O. Hansen, D. W. Higinbotham, T. Holmstrom, H. Ibrahim,

R. Igarashi, C. W. de Jager, E. Jans, X. Jiang, L. J. Kaufman, A. Kelleher, A. Kolarkar, G. Kumbartzki, J. J. LeRose, R. Lindgren, N. Liyanage, D. J. Margaziotis, P. Markowitz, S. Marrone, M. Mazouz, D. Meekins, R. Michaels, B. Moffit, C. F. Perdrisat, E. Piasetzky, M. Potokar, V. Punjabi, Y. Qiang, J. Reinhold, G. Ron, G. Rosner, A. Saha, B. Sawatzky, A. Shahinyan, S. Širca, K. Slifer, P. Solvignon, V. Sulkosky, G. M. Urciuoli, E. Voutier, J. W. Watson, L. B. Weinstein, B. Wojtsekhowski, S. Wood, X.-C. Zheng, and L. Zhu, Science **320**, 1476 (2008).

[16] H. Baghdasaryan *et al.* (CLAS Collaboration), Phys. Rev. Lett. **105**, 222501 (2010).

[17] I. Korover *et al.* (Jefferson Lab Hall A Collaboration), Phys. Rev. Lett. **113**, 022501 (2014).

[18] K. Miki, A. Tamii, N. Aoi, T. Fukui, T. Hashimoto, K. Hatanaka, T. Ito, T. Kawabata, H. Matsubara, K. Ogata, H. Ong, H. Sakaguchi, S. Sakaguchi, T. Suzuki, J. Tanaka, I. Tanihata, T. Uesaka, and T. Yamamoto, Few-Body Syst. **54**, 1353 (2013).

[19] H. Ong, I. Tanihata, A. Tamii, T. Myo, K. Ogata, M. Fukuda, K. Hirota, K. Ikeda, D. Ishikawa, T. Kawabata, H. Matsubara, K. Matsuta, M. Mihara, T. Naito, D. Nishimura, Y. Ogawa, H. Okamura, A. Ozawa, D. Pang, H. Sakaguchi, K. Sekiguchi, T. Suzuki, M. Taniguchi, M. Takashina, H. Toki, Y. Yasuda, M. Yosoi, and J. Zenihiro, Phys. Lett. B **725**, 277 (2013).

[20] M. Vanhalst, J. Ryckebusch, and W. Cosyn, Phys. Rev. C **86**, 044619 (2012).

[21] R. Weiss, B. Bazak, and N. Barnea, arXiv:1503.07047 [nucl-th].

[22] R. Schiavilla, R. B. Wiringa, S. C. Pieper, and J. Carlson, Phys. Rev. Lett. **98**, 132501 (2007).

[23] R. B. Wiringa, R. Schiavilla, S. C. Pieper, and J. Carlson, Phys. Rev. C **78**, 021001 (2008).

[24] R. B. Wiringa, R. Schiavilla, S. C. Pieper, and J. Carlson, Phys. Rev. C **89**, 024305 (2014).

[25] M. Alvioli, C. Ciofi degli Atti, L. P. Kaptari, C. B. Mezzetti, H. Morita, and S. Scopetta, Phys. Rev. C **85**, 021001 (2012).

[26] M. Alvioli, C. Ciofi degli Atti, L. P. Kaptari, C. B. Mezzetti, and H. Morita, Int. J. Mod. Phys. E **22**, 1330021 (2013).

[27] A. Fabrocini, F. Arias de Saavedra, and G. Co', Phys. Rev. C **61**, 044302 (2000).

[28] S. Bogner, T. Kuo, and A. Schwenk, Phys. Rep. **386**, 1 (2003).

[29] H. Feldmeier, T. Neff, R. Roth, and J. Schnack, Nucl. Phys. A **632**, 61 (1998).

[30] R. Roth, T. Neff, and H. Feldmeier, Prog. Part. Nucl. Phys. **65**, 50 (2010).

[31] S. K. Bogner, R. J. Furnstahl, and R. J. Perry, Phys. Rev. C **75**, 061001 (2007).

[32] S. Bogner, R. Furnstahl, and A. Schwenk, Prog. Part. Nucl. Phys. **65**, 94 (2010).

[33] E. D. Jurgenson, P. Navrátil, and R. J. Furnstahl, Phys. Rev. Lett. **103**, 082501 (2009).

[34] K. Hebeler, Phys. Rev. C **85**, 021002 (2012).

[35] R. Roth, A. Calci, J. Langhammer, and S. Binder, Phys. Rev. C **90**, 024325 (2014).

[36] M. D. Schuster, S. Quaglioni, C. W. Johnson, E. D. Jurgenson, and P. Navrátil, Phys. Rev. C **90**, 011301 (2014).

[37] H. Feldmeier, W. Horiuchi, T. Neff, and Y. Suzuki, Phys. Rev. C **84**, 054003 (2011).

[38] E. R. Anderson, S. K. Bogner, R. J. Furnstahl, and R. J. Perry, Phys. Rev. C **82**, 054001 (2010).

[39] S. K. Bogner and D. Roscher, Phys. Rev. C **86**, 064304 (2012).

[40] Y. Suzuki and W. Horiuchi, Nucl. Phys. A **818**, 188 (2009).

[41] J. Mitroy, S. Bubin, W. Horiuchi, Y. Suzuki, L. Adamowicz, W. Cencek, K. Szalewicz, J. Komasa, D. Blume, and K. Varga, Rev. Mod. Phys. **85**, 693 (2013).

[42] E. Caurier and F. Nowacki, Acta Phys. Pol. B **30**, 705 (1999).

[43] T. Neff, H. Feldmeier, W. Horiuchi, and D. Weber, (2015), arXiv:1503.06122 [nucl-th].

[44] M. Alvioli, C. Ciofi degli Atti, L. P. Kaptari, C. B. Mezzetti, and H. Morita, Phys. Rev. C **87**, 034603 (2013).

[45] K. Wendt, B. Carlsson, and A. Ekström, (2014), arXiv:1410.0646 [nucl-th].

[46] E. Epelbaum, H. Krebs, and U. G. Meißner, (2014), arXiv:1412.4623 [nucl-th].

[47] M. M. Sargsian, Phys. Rev. C **89**, 034305 (2014).

[48] O. Hen *et al.* (Jefferson Lab CLAS Collaboration), Science **346**, 614 (2014).

[49] G. Kamuntavičius, R. Kalinauskas, B. Barrett, S. Mickevičius, and D. Germanas, Nucl. Phys. A **695**, 191 (2001).

[50] P. Navrátil, Phys. Rev. C **70**, 014317 (2004).

[51] P. Navrátil, G. P. Kamuntavičius, and B. R. Barrett, Phys. Rev. C **61**, 044001 (2000).